

# METHODOLOGY AND SOFTWARE FOR GROSS DEFECT DETECTION OF SPENT NUCLEAR FUEL AT THE ATUCHA-I REACTOR

**KEYWORDS:** *spent nuclear fuel, gross defects, nuclear safeguards*

SHIVAKUMAR SITARAMAN,<sup>a\*</sup> YOUNG S. HAM,<sup>a</sup> NAREK GHARIBYAN,<sup>a</sup>  
ORPET J. M. PEIXOTO,<sup>b</sup> and GUSTAVO DIAZ<sup>c</sup>

<sup>a</sup>Lawrence Livermore National Laboratory, 7000 East Avenue, Livermore, California 94550

<sup>b</sup>Brazilian-Argentine Agency for Accounting and Control of Nuclear Materials, Avenida Rio Branco, 123/Grupo 515-Centro, CEP: 20040-005, Rio de Janeiro, Brazil

<sup>c</sup>National Regulatory Authority – Argentina, Av. Del Libertador 8250  
(1429) Buenos Aires, Argentina

Received July 10, 2014

Accepted for Publication February 5, 2015

<http://dx.doi.org/10.13182/NT14-63>

Fuel assemblies in the spent fuel pool are stored by suspending them in two vertically stacked layers at the Atucha Unit 1 nuclear power plant (Atucha-I). This introduces the unique problem of verifying the presence of fuel in either layer without physically moving the fuel assemblies. Given that the facility uses both natural uranium and slightly enriched uranium at 0.85 wt% <sup>235</sup>U and has been in operation since 1974, a wide range of burnups and cooling times can exist in any given pool. A gross defect detection tool, the spent fuel neutron counter (SFNC), has been used at the site to verify the presence of fuel up to burnups of 8000 MWd/t. At higher discharge burnups, the existing signal processing software of the tool was found to fail due to nonlinearity of the source term with burnup. A new software package based on the LabVIEW platform was developed to predict expected neutron signals covering all ranges of burnups and cooling times. The algorithm employed in the software uses a set of transfer functions that are coupled

with source terms based on various cooling times and burnups for each of the two enrichment levels. The software was benchmarked against an extensive set of measured data. Overall, out of 326 data points examined, the software data deviated from the measured data <10% in 87% of the cases. A further 10.5% matched the measurements between 10% and 20%. Thus, 97.5% of the predictions matched the measurements within the set 20% tolerance limit providing proof of the robustness of the software. This software package linked to SFNC will enhance the capability of gross defect verification at both levels in the spent fuel pool for the whole range of burnup, cooling time, and initial enrichments of the spent fuel being discharged into the various pools at the Atucha-I reactor site.

Note: Some figures in this paper may be in color only in the electronic version.

## I. INTRODUCTION

The Atucha Unit 1 nuclear power plant (Atucha-I) reactor is a pressurized heavy water moderated and cooled

reactor located in Lima, Argentina. It has a net capacity of 357 MW(electric) and has been in operation since 1974. The reactor started operations using natural uranium (NU) fuel while currently slightly enriched uranium (SEU) fuel at 0.85% <sup>235</sup>U is used. This has led to discharge burnups going from a range of 5000 to 8000 MWd/t to > 11 000 MWd/t. The active fuel length is 5.3 m with 37 active fuel

\*E-mail: [sitaraman1@llnl.gov](mailto:sitaraman1@llnl.gov)

rods clad in Zircaloy-4 arranged in three concentric rings, as shown in Fig. 1. The core contains 250 fuel assemblies arranged in a hexagonal lattice.

In the area of nuclear safeguards, the process of verifying the presence of spent fuel assemblies (SFAs) can prove challenging. This process, known as gross defect detection, is particularly the case with Atucha-I where SFAs are stored in six spent fuel pools each with two vertical storage layers. The assemblies are suspended from hangers (*perchas*) attached to large beams. Each pool has multiple beams with hangers from which SFAs can be suspended either on one side or on both sides of each beam. Routinely used visual tools such as the Digital Cerenkov Viewing Device are not effective even for the top layer since a large number of SFAs are in the low-burnup range and have cooling times of >20 years. This poses a unique problem of verifying the presence of fuel assemblies in the pool. Movement of the fuel is virtually impossible without removing large numbers of SFAs from their stored positions. This would be particularly the case for the lower layer of SFAs, which are also partially hidden from view looking down into the pool. It is therefore imperative to develop means of performing this verification in an in situ condition. Figures 2, 3, and 4 show the layout of the spent fuel in the fuel pools.



Fig. 1. Atucha-I fuel assemblies.

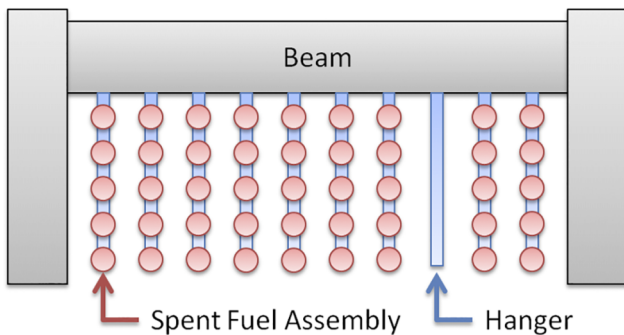


Fig. 2. Top view of single-side hanger for storing fuel assemblies.

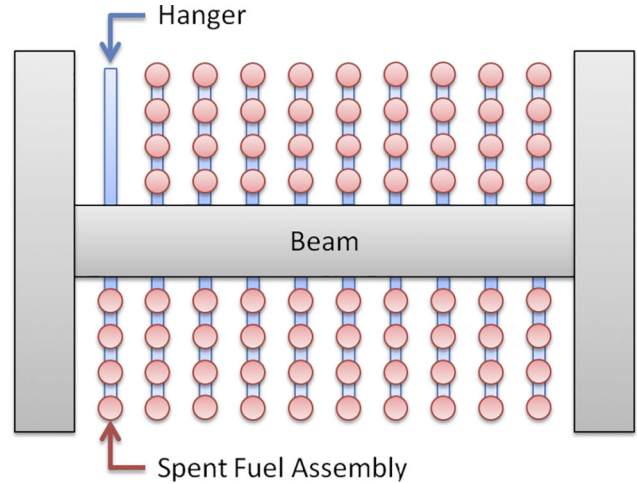


Fig. 3. Top view of dual-side hanger for storing fuel assemblies.

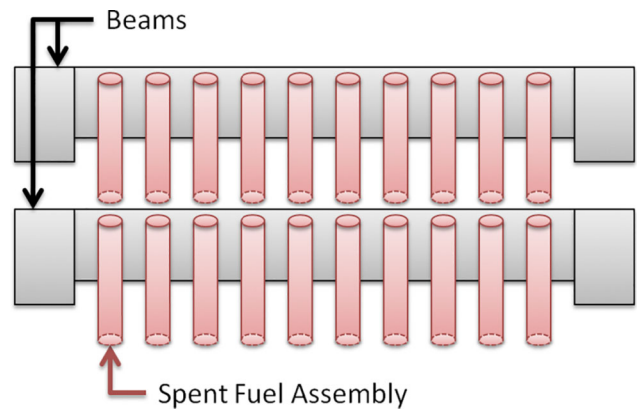


Fig. 4. Side view of hanger for storing fuel assemblies.

Figure 2 shows the top view of the configuration where assemblies are suspended from only one side. The alternate configuration of suspending assemblies from both sides is shown in Fig. 3. Last, Fig. 4 shows the axial view of the pool with the two layers of vertically stacked assemblies. Additionally, for both the single-side and dual-side configurations, there is the option of having low-density or high-density packing. Specifically, a single-side low-density configuration will suspend five assemblies per hanger while a high-density format will suspend six assemblies per hanger. In the case of the dual-side configuration, low-density packing will suspend four assemblies per side per hanger, while high-density packing will suspend five assemblies per side per hanger. It is important to note that the lower level of the pool does not necessarily copy the same hanger structure as the upper level and is not necessarily aligned. A dual-side low-density configuration can exist underneath a single-side low-density configuration, and both high- and low-density packing can be present at the same level. At both

enrichments the horizontal-to-vertical pitch for the low-density packing configuration in both levels is in the ratio 1:1. For the lower-level high-density configuration, this ratio is 0.91:1, and for the upper level it is 0.82:1. Aside from the special considerations of the physical arrangement of SFAs in the six storage pools, the SFAs have a wide range of burnups (5000 to 11 000 MWd/t) and cooling times (2 to 40 years) at both initial enrichments.

Early attempts at qualitative gross defect detection in the upper storage rack using a collimated CdTe detector were unsuccessful.<sup>1</sup> Meaningful  $^{137}\text{Cs}$  peaks were not obtained, and this technique for gross defect detection was abandoned. In 2002, a new system based on gross neutron counts was developed by the International Atomic Energy Agency<sup>1</sup> (IAEA). This instrument, the spent fuel neutron counter (SFNC), consisted of a fission chamber and a lead-shielded preamplifier covered with thick polyethylene. The whole assembly is placed in a water-tight stainless steel housing and is designed to fit snugly in the gap formed by four adjacent SFAs. In addition, an underwater viewing system consisting of a small camera was also used to position the instrument particularly in the lower level. The system used a mini multichannel analyzer as well as software that are both in fairly standard use at the IAEA. Figure 5 shows the SFNC in a spent fuel pool at the Atucha-I site. A linear calibration curve was constructed based on measurements using the SFNC that plotted the gross neutron counts versus the sum of the burnups of the four adjacent SFAs. In the event that an adjacent fuel assembly is a dummy, counts will not fall on the curve within a set tolerance indicating a gross defect. However, as the burnup of the SFA exceeded  $\sim 8000$  MWd/t, the linearity assumption breaks down. While not as nonlinear as light water reactor fuel, there is still sufficient nonlinearity in the pressurized heavy water reactor especially at lower cooling times. Thus, a new

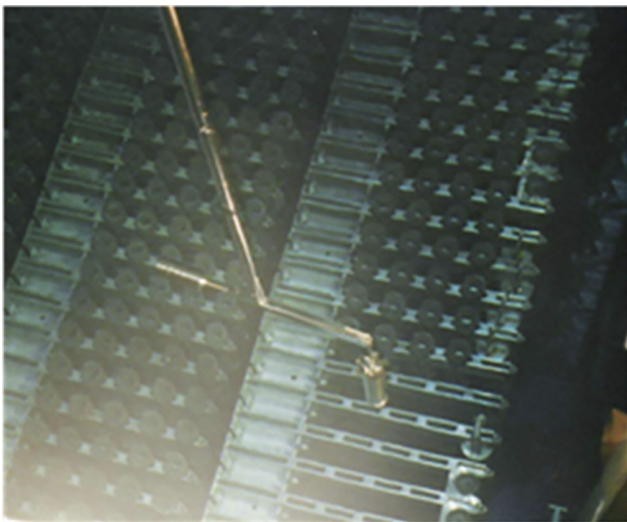


Fig. 5. Spent fuel neutron counter in a pool.

set of calibration curves would have to be developed in order to accommodate the whole range of burnups and cooling times of currently discharged SFAs. Instead of developing calibration curves, it was decided to develop maps of the expected signal at any location in a spent fuel pool covering all ranges of burnups and cooling times at both enrichments. To produce these maps a new algorithm and software were developed and benchmarked against a set of measurements taken in all the spent fuel pools.

The measurements used to benchmark the new software were taken over several days with individual counts of 120 s. This typically resulted in uncertainties of 1% to 2% in the counts. Multiple measurements were periodically taken at some locations to ensure repeatability of the data from the detector system. There was no detector pileup issue associated with these measurements that were taken over this short period of 120 s. Standard IAEA recommended procedures were used to determine the number of locations that was selected at each level of a pool. This involves using a formula that approximates the required sample size from the population that would result from a hypergeometric probability distribution (i.e., sampling without replacement).<sup>2</sup>

The following sections will discuss the methodology developed for this purpose, the software that was developed based on the methodology, the calibration of the software, and results from an extensive benchmarking exercise to validate the software.

## II. METHODOLOGY

The basic idea behind the methodology is to sum the expected contributions to the neutron count rate from nearby SFAs. This is illustrated by the diagram presented in Fig. 6. Given that the center spot is the measurement point, the predicted neutron count rate can be determined by adding all the contributions from each of the 36 nearby SFAs. In the layout where the horizontal and vertical spacing between assemblies is the same (Fig. 6a), each letter represents a unique  $(x, y)$  distance away from the center. In the layout of asymmetric horizontal and vertical spacing (Fig. 6b), there will be slight differences in the contributions from B and BB even if they have the exact same burnup and cooling time, due to their differing vertical and horizontal distances from the measurement point. Likewise, D will differ from DD, and E will differ from EE. The  $6 \times 6$  configuration is more than adequate to capture contributions from neighboring SFAs to the detector signal. Both symmetric and asymmetric layouts exist in the spent fuel pools at Atucha-I.

Earlier studies dealt with a methodology based on developing adjoint fluxes calculated using a hybrid stochastic-deterministic approach that can be used in conjunction with enrichment-, burnup-, and cooling time-based intrinsic source spectra to calculate the expected

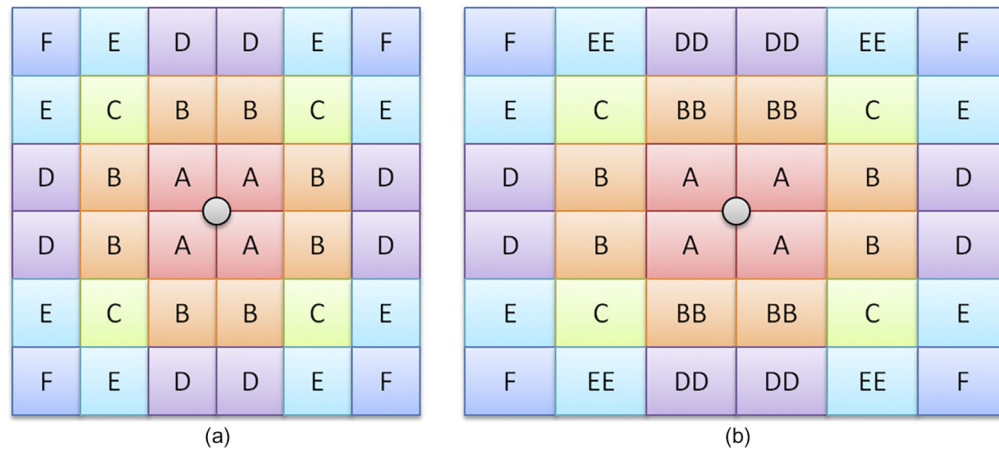


Fig. 6. The 6 × 6 grid of assemblies: (a) symmetric spacing and (b) asymmetric spacing.

signal at the detector location.<sup>3-6</sup> Burnup calculations to determine material composition and intrinsic neutron source were performed using the ORIGEN-ARP depletion code.<sup>7</sup> An extensive set of intrinsic source spectra in a standard BUGLE 47-group structure<sup>8</sup> was generated for the whole range of burnups and cooling times for each of the two initial enrichment levels used in the plant. Subcritical multiplication was modeled using a simplified fission-matrix method. Fission-matrix coefficients were determined using the MCNP code<sup>9</sup> for several burnups and decay times, which can be interpolated to obtain desired coefficients at different decay times and burnup levels. The total source was obtained by adding the multiplicative and intrinsic sources. The adjoint functions based on the interassembly pitches were generated for the SFAs in the vicinity of the detector using three-dimensional deterministic methods, and their respective sources were folded into these functions and summed to predict the signal at the detector location. However, since these data sets were constructed, the pool configurations at Atucha-I were changed. The adjoint fluxes are dependent on the distance between the sources and the detector. Since regenerating these fluxes together with the associated fission-matrix coefficients would be more time-consuming, a more straightforward, purely stochastic method was used to build source-to-detector transfer functions.

Radiation transport calculations were performed using MCNP for each interassembly pitch present in the various Atucha-I spent fuel pools. The basic methodology consisted of starting sources in each of the assemblies (e.g., A, B, BB, etc., as shown in Fig. 5) and tallying the contribution to the detector by a single neutron in each of the 47 energy groups used. These transfer functions in each group are multiplied by the actual intrinsic source strength in that group. The totals over each of the 47 groups for all 36 assemblies are then calculated, and the grand total over all the groups is the expected signal for that detector location. The calculations were performed with isotopics based on an average burnup of 8500

MWd/t and a cooling time of 20 years. The transfer functions are relatively insensitive to the isotopics used as described in the previously discussed studies involving the calculations of adjoint fluxes. The subcritical multiplication will be affected by the change in isotopics, and this was shown to be ~3% in the earlier study using the fission-matrix method.<sup>4</sup> However, given the uncertainties in the burnups and factors such as source linear interpolation in burnup and cooling time, etc., a realistic tolerance limit (see later discussion) will be applied, adequately covering any variations in the multiplicative source.

In order to calculate the predicted total neutron count rate, two sets of fixed data are required. A table of intrinsic source terms for each of the 47 energy groups is given for intervals of 1000 MWd/t burnups and ten selected cooling times between 0.03 to 40 years. The range of available burnups in the data sets is 4000 to 12 000 for NU and 9000 to 20 000 for SEU, in steps of 1000 MWd/t. The second set of data is a table of transfer functions that weights the contributions of each of the 47 energy groups depending on the SFA's distance from the point of measurement.

Linear interpolation is used to obtain the correct source spectrum at a specific burnup and cooling time. The use of linear interpolation to obtain a source term at intermediate burnups and cooling times differs from those obtained using fitted equations by 5% to 6%, with the interpolation being better in some instances than the fit. It is also noted that the methodology is based on folding the transfer functions in a 47-group structure into a 47-group neutron spectrum and that interpolation over both burnup and cooling time needs to be done for each energy group. The discharge burnups range from 5000 to a little over 11 000 MWd/t where a linear interpolation is an excellent approximation. This is especially important in the dominant energy groups between 1 and 2.5 MeV as well as between 4 and 5 MeV, where the difference with fitting is 1% to 1.5%.

### III. CALIBRATION OF PREDICTED SIGNALS

To convert the predicted neutron signals to more meaningful numbers, they are normalized by a calibration factor  $E$ . As described below, a set of  $n$  assemblies is chosen, and measurements  $x_i$  are taken with the SFNC, and the corresponding predicted neutron signal values  $r_i$  are calculated. Assuming the detector efficiency and measurement and calculational uncertainties can be rolled into a constant calibration factor, this calibration factor can be calculated by minimizing the square error function  $Y$ . This is done by taking the derivative of the function with respect to the calibration factor and setting it equal to 0 as shown in Eq. (1):

$$Y = \sum_i^n (x_i - E \times r_i)^2 \rightarrow \frac{d}{dE} \sum_i^n (x_i - E \times r_i)^2 = 0. \quad (1)$$

The resulting equation defines the calibration factor as the ratio of two sums. The dividend is the sum of the products between the measurement values and the corresponding predicted neutron count rate values. The divisor is the sum of the squares of the predicted values. This is shown in Eq. (2):

$$E = \frac{\sum_i^n (x_i \times r_i)}{\sum_i^n (r_i^2)}. \quad (2)$$

When the software is first deployed at Atucha-I, the initial calibration of the predicted database will be conducted. The operator supplies the inspectors with a map of the various pools containing information on the burnup, discharge date, and initial enrichment of each assembly and its location in the pool. The inspectors will have the pool maps from the previous verification campaign and can determine if anything has changed by way of arrangement of the spent fuel in the pools. Calibration of the software predicted signals will be required when this software is initially deployed at the site. Based on the properties of the various assemblies in each layer of each pool, the inspector will select four or five locations that reflect a good mix of the properties of the various assemblies, make measurements, and calculate a calibration factor. This factor is then applied to the predicted signal at each verification location selected by the inspector and compared to the measured signal to verify the presence of the spent fuel. It may be necessary to obtain more than one calibration factor in a single layer since the arrangement can be a mix of high- and low-density fuel stacking as in the case of pool 7, where three different calibration factors were needed in the lower level. Once these have been initially established, they are reused in subsequent verification campaigns by the inspectors. Calibration factors will have to be

reestablished if the detector system has been replaced or in the rare event that a pool configuration was changed by the operator through successive inspection campaigns. Even if the detector system and pool configurations have remained the same, calibration may have to be redone if a long time has elapsed between inspections, thus changing the cooling time of the spent fuel and impacting the source strengths. In this benchmarking exercise, four to five locations were used to establish calibration factors for each level in each pool. Per normal practice, the users will be given training on the use of the software in both the calibration and verification modes when it is deployed at the Atucha-I site.

With the calibration factor calculated, measurements can be taken using the SFNC in locations where the presence of SFAs needs to be verified. The predicted neutron signal values are also calculated for the corresponding locations, and calibration is then applied to all of the predicted values. Finally, these normalized predicted values can be compared to the measured values, and the deviation can be calculated by Eq. (3):

$$Deviation = \frac{(r_i \times E - x_i)}{r_i \times E}. \quad (3)$$

The objective of the verification is to determine if one or more of the four fuel assemblies adjacent to the detector has been replaced with a dummy assembly. The drop in signal strength per missing assembly is typically 24% to 27%. As an example, if such a drop is encountered—i.e., the predicted signal is larger than the measured one by approximately this value—the inspector will take more measurements to determine that the drop is genuine. By measuring in the neighboring locations with one or more of the assemblies from the suspect location still being adjacent to the detector and repeating this process as needed, the assembly that has been replaced can be identified.

Because the calibration factor minimizes the square error between the predicted neutron signal and the measured value from the SFNC, even applying the calibration factor on the original set of data will likely not produce exact matches. In addition, uncertainties with both the predicted and measured signals need to be factored into the process of determining the presence of the fuel assemblies. Therefore, a nonzero tolerance limit must be defined to determine whether or not a gross defect exists. Typical uncertainties are ~5% to 6% for the operator-declared assembly average burnup. Uncertainty in the source terms from ORIGEN are ~10% estimated from benchmark studies of the code. This value is based on the uncertainties in the estimation of the typical isotopic content of the principal neutron emitters,  $^{244}\text{Cm}$ ,  $^{240}\text{Pu}$ , and  $^{241}\text{Am}$ , as well as, to a much lesser extent, other Pu isotopes.<sup>10</sup> Interpolation versus curve

fitting conservatively adds another 5% to 6% uncertainty. The precision of the measurements is typically ~2% to 3% at the 2σ level, and repeatability of the measurement at the same location with small variations in the location is ~1% to 2% as determined from the benchmark measurements. The uncertainty in the transfer function sets is ~3%. The square root of the sum of squares gives an uncertainty of 14%. Thus, rounding up, a 15% value would constitute a minimum tolerance limit. However, since the signal drop from a replaced assembly is in the range 24% to 27% in the vast majority of situations, a 20% tolerance limit can be used at the upper end to provide added margin and still have the resolution to detect missing fuel. In rare instances where the four adjacent bundles have very different burnups and cooling times resulting in very different neutron source strengths, the removal of the assembly with the lowest source can result in a drop of only ~17%. In such cases, the lower limit tolerance limit of 15% will have to be set by the user. The benchmarking exercise in this study used the upper 20% tolerance limit.

**IV. APPLICATION SOFTWARE**

Having established a methodology, the next step was to link it to the SFNC by developing a software package. Practical considerations in the form of ease of use by nuclear inspectors are of primary importance in developing the software. In light of this, the LabVIEW commercially available platform<sup>11</sup> was used to build graphical user interface (GUI) software modules that used operator-declared databases of burnup and cooling times to predict expected signals at any location in the various spent fuel pools at the site. A step-by-step approach with a very clear and visual interface was implemented to minimize user error. The main screen is shown below in Fig. 7. The left side presents the user with the current progress. The bottom bar allows the user to restart, read the help screen, or quit, at any time. The software compares the expected signal to the measured one and alerts the inspector if the deviation is beyond the user set tolerance limit.

As shown in Fig. 7, prior to first use, calibration factors need to be generated for the various configurations present in a pool. This is done by exercising the calibration option, which steps through the various screens that allow the operator to choose a set of locations and calculate a calibration factor based on measured signals at each location. At the end of this process, a text file is created and saved for use during the verification process. Figure 8 illustrates a screen at the end of the calibration step showing a calibration factor. As discussed earlier, new calibration factors can be derived at the discretion of the user based upon changes in a pool configuration or cooling times and changes in hardware.

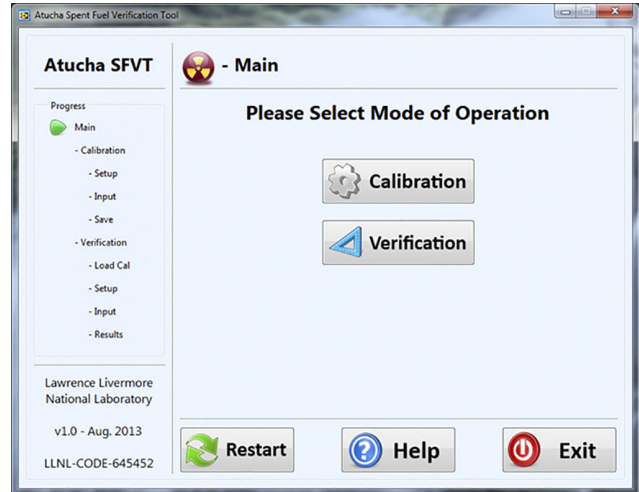


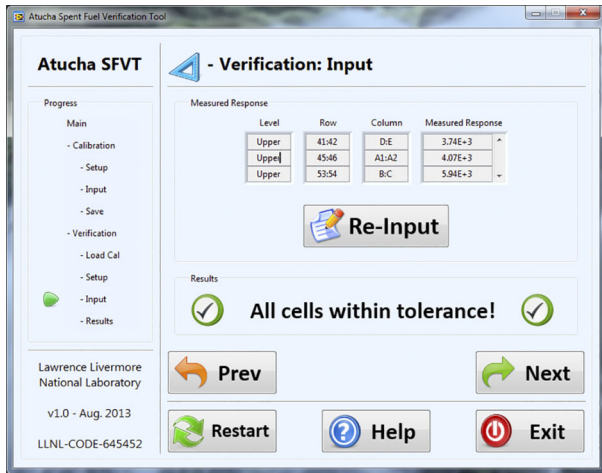
Fig. 7. Opening screen of the GUI software.



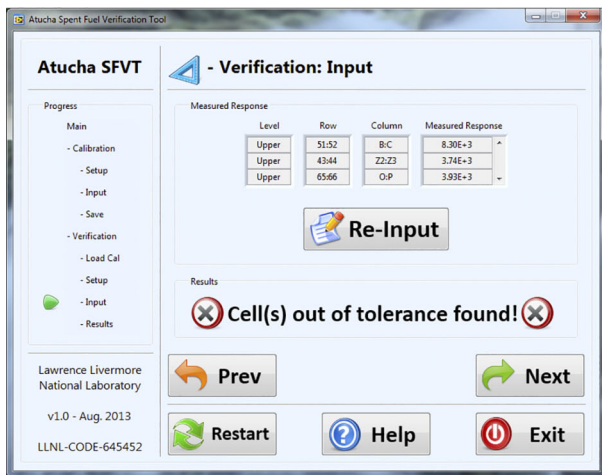
Fig. 8. Calibration factor calculation completed.

During a verification campaign, the first step would be to exercise that option (see Fig. 7) and call up the appropriate calibration file. Similar to the calibration process, the user selects inspection locations and steps through the various screens to obtain the expected signal that is then compared to the measured signal. The deviation of the expected signal from the measured one is displayed, and the inspector is informed as to whether all signals are within the set tolerance or not. Figure 9 shows examples of each of these situations. Any deviation outside the tolerance may require further action by the inspector.

The software was then benchmarked against an extensive set of data that was taken at the various pools in 2004. The results of this benchmarking exercise are discussed in Sec. V.



(a)



(b)

Fig. 9. Verification complete: (a) within tolerance and (b) out of tolerance.

**V. BENCHMARKING OF SOFTWARE**

A set of 335 measurements was taken jointly by the Brazilian-Argentine Agency for the Accounting and Control of Nuclear Materials and the IAEA in 2004. This set was selected out of a total of 8719 SFAs that were present in all the pools at the time of the 2004 measurement campaign. This extensive set of measurements covered both levels of five of the active pools with a small set of data at the lower level in pool 5. The set included a wide range of cooling times and burnups at both enrichment levels and various interassembly pitches. In addition to measurements in the midst of four SFAs, there were a few measurements taken at locations with only two SFAs present in the immediate vicinity of the SFNC. Calibration factors were derived for each pool at each level and for each of the pitches that existed in these levels. Sections V.A. through V.F compare the measured and predicted data for each of the six pools. As mentioned

earlier, a tolerance level of  $\pm 20\%$  was set for these comparisons.

**V.A. Pool 1**

There were 61 measurements taken in pool 1 with 28 of these at the upper level and the rest at the lower level. Figure 10 compares the measured and predicted counts for this set. Of the 59 points examined, 50 data sets were within 10% of each other with 7 points in the 10% to 20% range with one of these just within the 20% mark. Two points fell outside the tolerance limit. On examining these two points, the measured data were very different from those at similar burnups and cooling times in the vicinity. The cause of this discrepancy was investigated, but the measurement logs did not shed any further light on this issue. Two measurements were taken at locations with two SFAs at the edge of the pool. These two measurements were taken between two SFAs next to the edge of the pool. However, this is not a usual location where measurements are taken, and detection of fuel at the edge can be accomplished by moving the detector location to the space between the two assemblies close to the edge and the two assemblies located in a once removed position from the edge. Other locations that did include pool edge row or column spent fuel were within tolerances since these measurements were performed at the usual location that consisted of two assemblies at the edge and two once removed from the edge where existing transfer function data are adequate for the analyses.

**V.B. Pool 2**

There were 52 measurements in this pool with 20 of those in the upper level and the rest in the lower level. Figure 11 presents the comparison for his pool. The predicted data matched the measured data in 40 instances

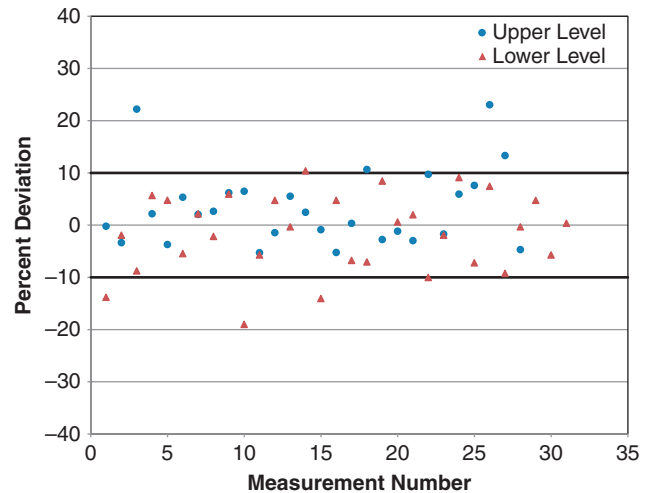


Fig. 10. Comparison of measured and predicted signals: pool 1.

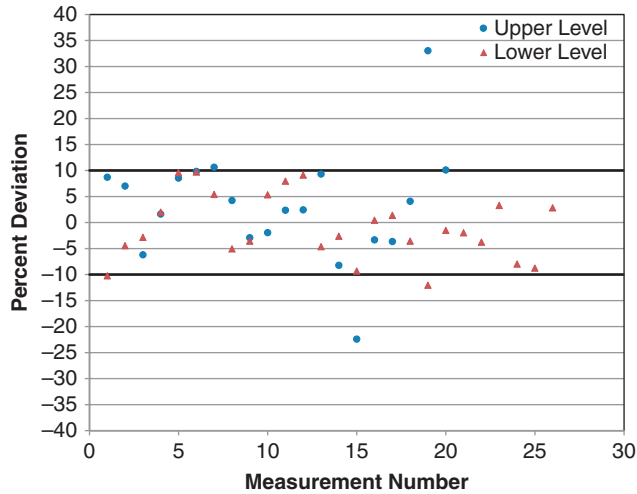


Fig. 11. Comparison of measured and predicted signals: pool 2.

with four data points falling in the 10% to 15% range. Two points were beyond the 20% range with one of these well over 30%. The predicted value in the latter was much higher, and once more, examination of the measurement records did not shed any further light on this issue. One of the 52 measurements was in a location surrounded by four empty slots, an unusual measurement, and was not included in the benchmarking exercise. There were five measured points with unusually high counts that were about twice the value compared to similar locations in the pool that are not shown in Fig. 11. Records from the inspection on these locations do not contain any further information on these such as specifically whether the counting time was doubled from what it was for the rest of the measurements. The records do only indicate that these measurements were made on a different day from the others. By halving the counts, the predicted and measured signals are within 10% of each other. However, in light of the uncertainties surrounding these measurements, they were excluded from consideration.

**V.C. Pool 4**

This pool had 64 measurements, and the comparisons are shown in Fig. 12. The measured and predicted data were within the 10% range for all but five data points. Three of these data points were in the range 10% to 15%, and one point was between 15% and 20%. One point in the lower level exhibited a large difference. Here again, the measured value was very much larger when compared to data from similar locations in the pool.

**V.D. Pool 5**

This pool had very limited measured data in the lower level and no data in the upper level. Seven of the nine data points shown in Fig. 13 were within the 10% range with the remaining two between in the 10% to 15% range. Pool

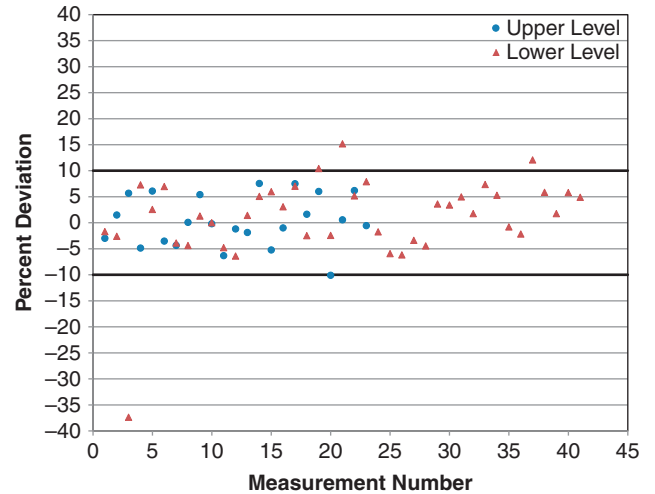


Fig. 12. Comparison of measured and predicted signals: pool 4.

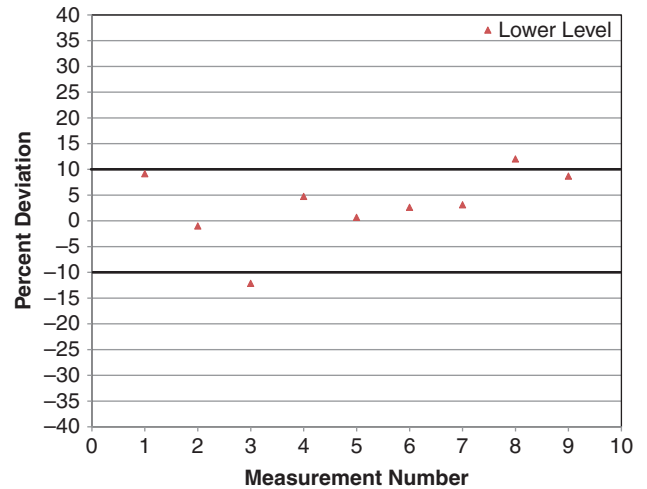


Fig. 13. Comparison of measured and predicted signals: pool 5.

5 had only 208 assemblies in the lower level, and nine locations were selected based on the standard IAEA criterion for picking the sample size discussed earlier in this paper.

**V.E. Pool 6**

This pool had a total of 71 measurements: 34 in the upper level and 37 in the lower level. The measured and predicted data, presented in Fig. 14, were within the 10% range for 62 of these points with an additional 5 in the 10% to 15% range. Of the remaining four data points, three were within the 15% to 20% range, and one was just over the 20% level.

**V.F. Pool 7**

This was the most complex pool since it had a mix at both levels of initial enrichment as well as mixed

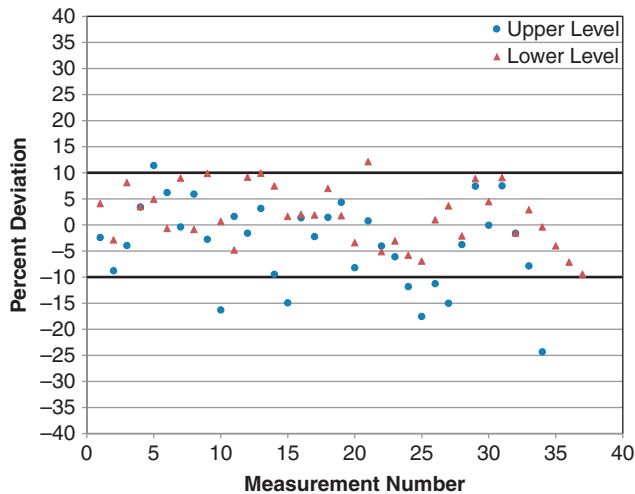


Fig. 14. Comparison of measured and predicted signals: pool 6.

interassembly pitches. It required three calibration factors to accommodate these differences in the lower level. Figure 15 presents a total of 78 points at both levels. Of these, a total of 65 points were within the 10% range. Seven more points fell in the 10% to 15% range with three in the 15% to 20% range. Two points were outside the 20% tolerance level, and a third one was off scale in Fig. 15. This latter point had a measured value about twice the signal levels from similar locations in the vicinity.

**V.G. Summary of Benchmarking**

In summary, 283 of the predicted signals, representing 87% of the total of 326 points considered in the benchmarking exercise, matched the measured data within  $\pm 10\%$ . A further 27, or 8%, were in the range of  $\pm 10\%$  to 15%, and 8, or 2.5%, were in the range of  $\pm 15\%$  to 20%. Thus, 97.5% of the data matched the measurements

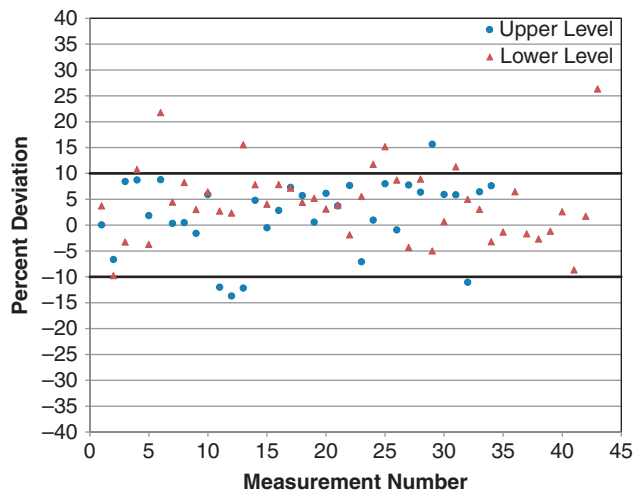


Fig. 15. Comparison of measured and predicted signals: pool 7.

within the set tolerance limit of 20% with 95% matching measured data with the lowest allowed tolerance limit of 15%. Eight data points were outside the tolerance limit with all of them having measured values that were very different from those in their vicinity with similar burnup and cooling times. Causes for this could be wrongly entered data or wrong burnup/cooling time information in the operator declaration of these properties of the surrounding SFAs. As discussed earlier, six points were not considered in the benchmarking exercise since they were anomalous in that they were very much larger than the expected values based on several measurements in the vicinity with very similar spent fuel properties. Further clarification of the cause of these discrepancies was investigated with the examination of the inspection records. However, this did not shed any further light on the cause of these discrepancies. Finally, three points were excluded since these were at the edge of the pool that were either in atypical positions or in an empty slot (i.e., all four adjacent assemblies were missing).

**VI. CONCLUSIONS**

The new software package that has been developed will be linked to the gross defect detection tool, SFNC, and deployed at the Atucha-I site. The GUI software is designed for ease of use and maps expected neutron signals at various locations within the spent fuel pools where fuel is stored in two vertical layers. Comparison of the predicted and measured signals at any location within these pools will enable inspectors to detect gross defects. The software has been benchmarked against an extensive set of measured data and found to be robust and reliable. The deployment of this software package will enhance the reliability of the spent fuel safeguards measurements at the facility.

**ACKNOWLEDGMENTS**

This work was performed under the auspices of the U.S. Department of Energy (DOE) by Lawrence Livermore National Laboratory under contract DE-AC52-07NA27344. The authors wish to thank DOE International Nuclear Safeguards and Engagement Program NA241 for its support for this work. The authors also wish to thank Nucleoelectrica Argentina S.A. for its valuable contribution to this project.

**REFERENCES**

1. Y. HAM et al., "Neutron Measurement Techniques for Verification of Closely Packed Spent Fuel Assemblies Stored in a Spent Fuel Pond," *Proc. INMM 44th Annual Mtg.*, Phoenix, Arizona, July 2003, Institute of Nuclear Materials Management (2003).
2. *IAEA Safeguards Glossary—2001 Edition*, International Atomic Energy Agency, Vienna, Austria (June 2002).

3. W. WALTERS et al., "Methodology and Determination of Field of View of Neutron and Gamma Detectors in the Atucha Spent Fuel Storage Pool," *Proc. INMM 50th Annual Mtg.*, Tucson, Arizona, July 2009, Institute of Nuclear Materials Management (2009).
4. W. WALTERS et al., "Calculation of Sub-Critical Multiplication Using a Simplified Fission Matrix Method," *Trans. Am. Nucl. Soc.*, **101**, 447 (2009).
5. W. WALTERS et al., "A Methodology for Determination of Detector Response for Inspection of a Spent Fuel Pool," *Proc. PHYSOR 2010—Advances in Reactor Physics to Power the Nuclear Renaissance*, Pittsburgh, Pennsylvania, May 9–14, 2010, American Nuclear Society (2010).
6. S. SITARAMAN et al., "In-Situ Verification of Spent Fuel at the Atucha-I Nuclear Power Plant," *Proc. INMM 52nd Annual Mtg.*, Palm Desert, California, July 2011, Institute of Nuclear Materials Management (2011).
7. "ORIGEN-ARP, Version 5.1.01, Isotope Generation and Depletion Code," CCC-732, Radiation Safety Information Computational Center (Mar. 2007).
8. J. E. WHITE et al., "BUGLE-96: A Revised Multi-Group Cross Section Library for LWR Applications Based on ENDF/B-VI Release 3," *Proc. Topl. Mtg. Radiation Protection and Shielding*, Falmouth, Massachusetts, April 21–25, 1996, Vol. 2, p. 1071, American Nuclear Society (1996).
9. X-5 MONTE CARLO TEAM, "MCNP—A General Monte Carlo N-Particle Transport Code," Version 5.1.40, Los Alamos National Laboratory (Feb. 2006).
10. A. PAVELSCU et al., "CANDU Radiotoxicity Inventories Estimation—A Calculated Experiment Cross-Check for Verification and Validation," *Romanian J. Phys.*, **52**, 1–2, 137 (2007).
11. "LabVIEW 2012-A System Design Platform," National Instruments.